Study of the Crystalline State of MBE (013)HgCdTe/CdTe/ZnTe/GaAs Heterostructure Layers by the Second Harmonic Generation Method

© S.A. Dvoretsky[1,4], M.F. Stupak[2], N.N. Mikhailov[1,3], S.N. Makarov[2], A.G. Elesin[2], A.G. Verhoglyad[2]

[1] Rzhanov Institute of Semiconductor Physics, Siberian Branch, Russian Academy of Sciences,
630090 Novosibirsk, Russia
[2] Technological Design Institute of Scientific Instrument Engineering at the Siberian Branch
of the Russian Academy of Sciences (TDI SIE SB RAS),
630058 Novosibirsk, Russia
[3] Novosibirsk State University,
630090 Novosibirsk, Russia
[4] Tomsk State University,
634050 Tomsk, Russia

E-mail: dvor@isp.nsc.ru

Received March 2, 2022
Revised March 25, 2022
Accepted March 25, 2022

The crystal perfection of HgCdTe layers of heterostructures grown on (013)GaAs substrates with ZnTe and CdTe buffer layers and orientation rotation in the plane(angle φ) and perpendicular to the growth direction (angle θ) were studied by the method of second harmonic generation. A change in the angle φ for CdTe layers was observed depending on the GaAs substrate orientation and its non-monotonic change throughout thickness in the MCT layer of constant composition and graded widegap layers at its boundaries. An increase in the angle θ was observed when growing the upper graded widegap MCT layer. The absolute value of the angle θ can be used for a qualitative assessment of the crystalline perfection of the HgCdTe layers.

Keywords: crystals of the sphalerite class, second harmonic, azimuthal angular dependencies, crystal perfection, $Cd_xHg_{1-x}Te$ heterostructures.

DOI: 10.21883/SC.2022.08.54114.31

1. Introduction

The heteroepitaxial structures (HES) of the solid solution of the mercury cadmium telluride (MCT, $Hg_{1-x}Cd_xTe$) being grown by the molecular beam epitaxy (MBE) take a leading position as a basic photosensitive material for IR detectors with high sensitivity within a wide spectra wavelengths range [1,2]. A promising field is regarded to be application of MCT HES'es for the IR and terahertz (THz) laser as well as the THz detectors of the spectrum ranges of the wavelengths [3–5]. The photovoltaic characteristics of the devices based on MBE MCT HES'es are to a large extent determined by the crystal perfection of the structure. The studies were performed to show that the MBE MCT HES'es of an device quality and high structural perfection are grown by using the substrates with a vicinal surface (112)B and (013) (see [6] (and references therein), [7–9]). As it is known, due to the mismatch of crystal lattice parameters (CLPs), the occurring stresses result in generation of mismatch dislocations (MD) and the increase in the density within a growing layer (with the increase in the thickness the stress increases to the critical value and a dislocation net is formed for stress relief). The growth of MBE MCT HES'es with a molar content $X_{CdTe} \cong 0.22$ cadmium telluride on the $Cd_yZn_{1-y}Te$ ($y = 0.04$) isovalent substrates with full compliance of the CLPs of the MCT layer and the substrate makes it possible to ensure the maximum structural perfection of the structures [10–12]. However, the insignificant difference of the CLPs results in the degradation of structural perfection and the increase in the density of threading dislocations dens. The growth of MBE MCT HES'es on the alternative substrates Ge, GaAs and Si with the large mismatch of the CLPs of the MCT layer and the substrates results in significant (about 2 orders and more) dislocations density increase. Also, the growth on the vicinal surfaces results in the rotation of the growing layer orientation within the plane and in the growth direction in relation to the specified orientation of the substrate, which are related to the CLP difference, type and number of dislocation in the substrate [13,14]. Most commonly, the angles of the layer orientation rotation in relation to the substrate along the growth direction during the HES growth are experimentally measured by the X-ray diffraction method. The rotation of the orientation plane along the growth direction is observed when growing the heterosystems based on the various semiconductors [15–22]. For the MBE MCT HES'es on the (112)CdZnTe substrate, there was evidently the rotation of the orientation plane to 100 ang. s with the insignificant CLP mismatch of 0.116% [10]. For the MBE MCT HES'es, there was evidently the rotation of the (111)CdTe plane by 2−6 angl. deg. with deflection of the (001)GaAs substrates by 2−7 angl. deg. [23]. The study [24] reports the rotation by 3.5 angl. deg. of the

(112)CdTe layer plane when growing on the (112)ZnTe/Si substrate. The detailed studies of the orientation rotation of the (013)CdTe and (013)HgCdTe layers when growing on the (013)ZnTe/GaAs(Si) substrates and the mechanisms dislocations introduction are given in [25]. The rotation (013)CdTe plane layers was 0.68–1.59 angl. deg. and 2.31–4.4 angl. deg. when growing on the (013)ZnTe/Si and (013)ZnTe/GaAs substrates, respectively. The main cause of the rotation along the growth direction is related to the CLP mismatch in the pseudomorphic growth [17] or to the introduction of edge mismatch dislocations [13]. In addition to the introduction of edge dislocations, it is possible to introduce the screw dislocations, which define the surface rotation within the growth plane [13].

Taking into account a unique determinability of the absolute orientation for non-centrosymmetric crystals in relation to the shear plane by the second harmonic generation of the probing laser radiation, we have examined the rotation of the orientation of the (013)GaAs substrates and the (013)CdTe layers when growing on the (013)ZnTe/GaAs substrates within the growth plane by the second harmonic generation (SHG) [26–29]. It was shown that for the CdTe/ZnTe/GaAs(013) structures the rotation within the growth plane was from 3 to 8 angl. deg and depended on the rotation of the initial GaAs substrate surface from (013). The SHG can be used to perform express contactless measurements of the structural perfection of the crystal without an inversion center with the high local resolution in thin subsurface layers [30]. For the GaAs crystals, the epitaxial CdTe layers on the various substrates and the MBE MCT HES'es on the GaAs and Si substrates the SHG method has demonstrated the high efficiency and allowed obtaining new data in measuring the crystal perfection [31–33].

The second harmonic generation (SHG) is a faster and more convenient method in comparison with the electron and X-ray diffraction methods in the studies for obtaining the express non-destructive information, which supplements the application of traditional electron, X-ray and other diffraction methods [26–29,34–40].

The present article presents the results of highly-sensitive SHG studies of the crystal state of the (013)HgCdTe/CdTe/ZnTe/GaAs heterostructures and the rotation of the (013) orientation in the azimutal plane and in the perpendicular growth direction in various layers of the heterostructure and throughout the HgCdTe layer thickness.

2. Samples and experimental procedure

The SHG studies of the structural perfection and the orientation plane rotation in two MBE MCT HES were carried out. The samples were grown by the MBE with control of the layer composition and thickness by single-wave ellipsometry *in situ* [41]. The (013)GaAs substrates polished on both sides were used for the

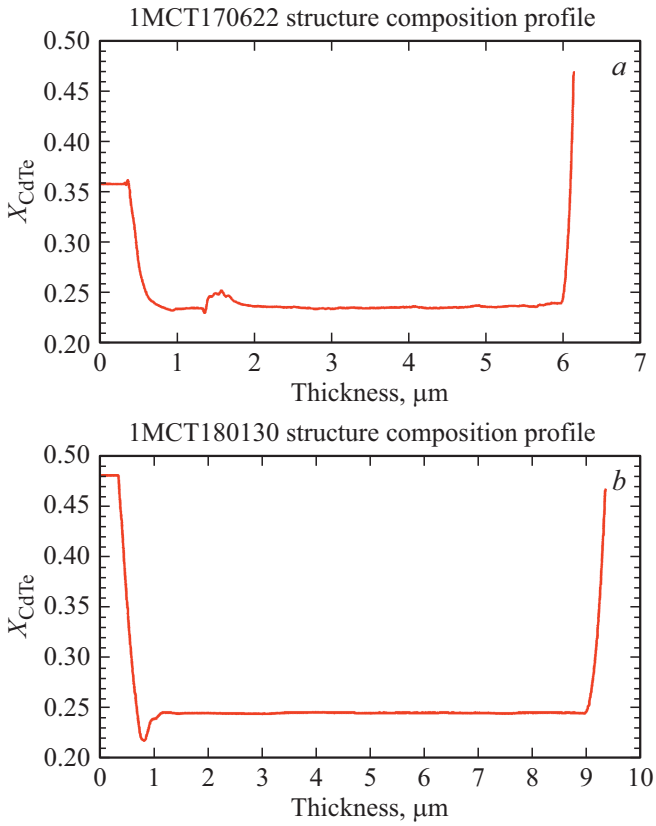

Figure 1. Composition distribution X_{CdTe} within the MBE MCT HES layers: *a* — 1MCT170622, *b* — 1MCT180130. The surface of the left substrate is defined by a zero coordinate of the horizontal axis.

MBE MCT HES growth. To maintain the orientation and to resolve the issue of a large 13.6% mismatch between the GaAs lattice and MCT parameters, ZnTe and CdTe buffer layers are grown sequentially. The new „alternative“ CdTe/ZnTe/GaAs substrate maintains the (013) orientation and ensures a significantly smaller mismatch of the lattice parameters with MCT ($< 0.3\%$). The grown structures include the ZnTe and CdTe buffer layers and the MCT layer with graded-gap wide-band layers at the heterogeneous layer interfaces on the (013)GaAs substrate. The thicknesses of the ZnTe and CdTe layers were up to 30 nm and 5.5 μm, respectively. Fig. 1 shows the composition profile inside the MCT layers of the MBE MCT HES structures 1MCT170622 and 1MCT80130.

The MCT layers with the homogeneous composition ~ 0.23 for structure 1MCT170622 and $x \sim 0.24$ for structure 1MCT180130, of the thickness of 5–8 μm included the lower wide-band graded-gap layer at the heterointerface with the CdTe buffer layer with the composition changing from $x \sim 0.45$ to $x \sim (0.23–0.24)$ of thickness $\sim 1.5\,\mu$m and the upper wide-band graded-gap layer with the composition changing from $x \sim (0.23–0.24)$ to $x \sim 0.4$ of a thickness $\sim 0.5\,\mu$m on the MCT surface.

The structural crystal perfection of the substrate and the MBE MCT HES layers was measured at the room temperature by the SHG method *ex situ* on the high-sensitive laboratory test bench for the non-linear optical diagnostics, which operation is described in detail [27,28]. The average power for SHG was changed within the range 0.01 to 0.07 W by means of the Nd : YAG-laser. The azimuthal dependence measurement range of the second harmonic (SH) signal from 10 s to 30 s.

The noise value (with zero mean) corresponded to ~ 16 ADC code unit, while the characteristic amplitude level of the SH signal in the diagrams was ranged within 2000−4500 ADC code units. The experimental SH signal amplitudes (along the surface or for the same-type samples) can be comparatively analyzed with an error below 0.05. The SH polarization components dependence intensity on the mutual orientation of the polarization of excitation radiation in reference to the crystallophysical axes was measured, whereby the experiment recorded the SH polarization parallel to the azimuthally changing linear polarization of the excitation radiation (hereinafter referred to as the azimutal dependence). The experimental and numerical model data for the ideal crystal in a given local area were analyzed to obtain the quantitative information about the crystal state of the subsurface layer, its orientation and the growing layers orientation rotation within the plane and the growth direction, as well as a number of other characteristics with an error no worse one degree [26–29,34–40]. The crystal state of the MCT layers was measured by azimuthal SH signal intensity dependence measurement with layer-by layer etching. We experimentally established that the SH signal amplitude and structure do not depend on the surface etching, which enabled establishing regularities of the (013) surface behavior when growing a complex multi-layer HgCdTe/CdTe/ZnTe/GaAs structure.

3. Results and analysis of experimental data

3.1. Analysis of the behavior and recording of the azimuthal dependences of the second harmonic signals in the GaAs, CdTe, HgCdTe crystals near the (013) orientation

The SH calculation using the non-linear susceptibility tensor $\chi_{xyz}(\omega)$ in the crystals of sphalerite or zinc blende (international classification — class $\bar{4}3m$) is described in detail in [30,31]. When comparing the calculation and experimental results of the azimuthal SH signal dependences in a specific geometry and for specific crystal slices, numerical modelling is applied [25–29,32–34].

The GaAs substrate and the CdTe and ZnTe layers are transparent within the excitation radiation region $\sim 1\,\mu$m [37–39]. The penetration depth of the SH radiation (wavelength $\lambda = 0.53\,\mu$m) in the field of fundamental absorption for CdTe, GaAs and ZnTe is equal to 130 nm, 140 nm and 210 nm, respectively accoding out data and agrees with [42–44]. The MCT layers are opaque both for the excitement radiation at $\lambda = 1.064\,\mu$m, and for its second harmonic. According to our data, the penetration depth for the upper wide band graded-gap layer of the studied heterostructures in terms of an amplitude radiation with wavelength $\sim 1\,\mu$m does not exceed $0.2\,\mu$m, while the SH absorption length in terms of the amplitude is $\leq 0.03\,\mu$m, thereby well agreeing with the data of the studies [43,44]. This means that in our experiments, the SH signals from the MCT heterostructure and from its rear side (the GaAs substrate) are purely reflected.

In case of a transparent medium, the effective depth the reflected second harmonic generation is determined by its coherent length $d \approx \lambda/4\pi n(\omega)$, while in strong absorption the generation depth d is defined by the minimum value of the magnitudes $\alpha^{-1}(\omega)$ and $\alpha^{-1}(2\omega)$ [25], where λ is the wavelength of the main radiation, $n(\omega)$ is the refraction index of the medium at this wavelength, α is the absorption coefficients at the basic and double frequencies. In case of weak absorption $d = \lambda/4\big(n(\omega) + n(2\omega)\big)$ [45,46]. The performed evaluations showed that the SHG diagnostics depth of the studied HgCdTe samples was determined by the magnitude $\alpha^{-1}(2\omega)$, the generation depth of the second harmonic reflected from the GaAs substrates and the CdTe layers (without taking into account the laser radiation reflected from the opposite side) was determined by the coherent length to be $\sim 20-25$ nm.

The analysis of the curves behavior of the model azimutal dependences of the SH signal with the variation by the angles θ and φ near the (013) orientation showed (see studies [26–29]) that these dependences are very sensitive to small deviation from the angle φ at the normal beam incident. That is why the laboratory test bench was used to perform the normal incidence of the laser radiation of frequency ω to the studied sample by simultaneously rotating its polarization plane (azimuthal angle) within the range from 0 to 359° and recording the intensity reflected second harmonic signal with the polarization parallel to the polarization of the laser radiation.

The curve of the azimuthal dependence of the second harmonic signal for the ideal orientation (013) should demonstrate the same amplitudes of all the four maximums (Fig. 2).

Fig. 2 shows the model azimuthal dependences of the SH reflected signal on the angle φ variation near the (013) for the crystals of the $\bar{4}3m$ class. The angles θ and φ data for (013) were determined by deviation from (100) in the simulation. Here, the polarization intensity signal of the reflected second harmonic is parallel to the polarization of the exciting laser radiation. The bold dark line represents the curve of the azimuthal SH signal dependence for the perfectly accurate orientation (013) at the angle $\varphi = 90°$, which shows the same amplitudes of all the four maxima.

The thorough analysis of our many experiments with the MCT structures and substrates around the (013) orientation [27–29] can be used to make an unambiguous

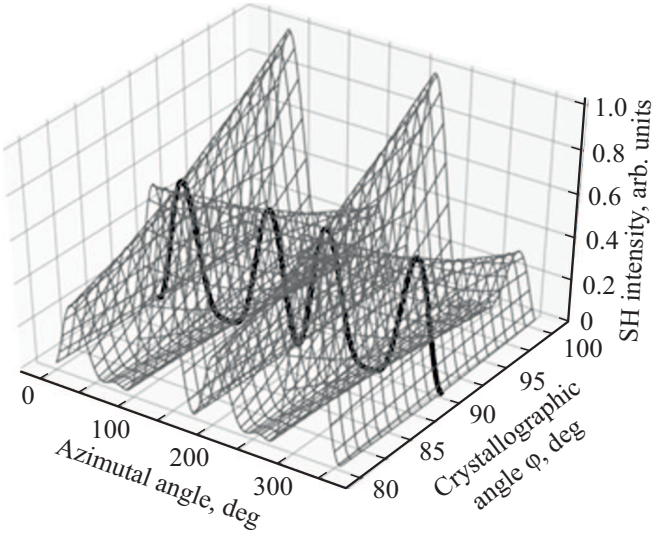

Figure 2. Model surface of the azimuthal SH intensity for the normal beam incident with shear variation near (013) by angle φ. The SH signal polarization is parallel to the polarization of the exciting radiation.

conclusion that the express diagnostics, by the SH signal, of the absolute orientation for the local area of the studied sample by the angle φ (with the error, if necessary, up to 0.1 degrees of arc) is totally reliable and does not require any additional checks.

The angle θ determines the deviation of the direction of the substrate orientation from the direction of the (001) planes in the zinc blende structure. For the (013) orientation, this angle is 18.46 angl. deg. It was demonstrated [27–29] that the SH signal variations for the θ angle (at fixed angle φ) near the (013) orientation result in the simple change of the amplitude in the maxima of the SH intensity curves on the azimuthal angle without changing the ratios between the maxima.

The amplitudes variation of the two adjacent maximum of the model azimuthal SH signal dependences around the angle $\theta \approx 19$ angl. deg. (Fig. 3) was additionally analyzed to show that with the increase in the angle θ by 8 angl. deg. the SH signal amplitude linearly increases two times depending on the variation of angle θ. The dots of Fig. 3 show the linear dependence of the amplitude of equal SH maxima on the angle θ with the slope tangent 0.25 at the ideal orientation (013) for angle φ. As it is clear in Fig. 3, the same linear dependences for the respective maxima are obtained at the deviation from (013) for the fixed angle φ.

It means that without control of the SH signal amplitude, in the experiment with the same-type zinc blende structure samples, the error of SHG determination of the angle θ near the (013) orientation can be up to ± 5 degrees of arc. If the series of the experiments exhibits the insignificant differences of the SH signal amplitudes from various surfaces of the single-type studied structures, then it suggests that the variations of angle θ are within the maximum of 2–3 angl. deg.

For the semiconductor materials and structures, which are transparent for the basic radiation, the recorded signal value of the combined (reflected plus passed) second harmonic at the specified level of the exciting laser radiation is determined to a greater extent by re-reflection of the exciting radiation from the rear sample surface [26–28,34]. When studying the GaAs substrates and the CdTe buffer layers on those substrates, the SH signal corresponds to a point group of the crystal subsurface layer symmetry and thus, can be used for characterization of the 0.3–1 μm thick layer structural quality. The SH signal value in this case may exceed, by an order, the SH signal value [26,27,34] reflected from the front surface only.

Since the MCT layers are opaque for the exciting radiation ($\lambda = 1.064\,\mu$m) and for its second harmonic, the experiment fixes only the reflected SH both from the surface MCT layer and from the rear substrate side. In our experiments, the GaAs had two-sided polishing. This is allows to comparatively analyze the non-linear susceptibilities of these materials, to diagnose the comparative presence of the stresses in the substrate or in the layers of the MCT heterostructure as well as to determine with a high accuracy the difference in the layers orientation of the MCT heterostructure and the GaAs substrate for angle φ.

It should be noted that the presence of the stresses is easily detectable by SHG in the substrate and their threading into the layers of the MCT heterostructure being grown [28] eventually results in some insignificant increase in the errors orientation determination for the angles θ and φ.

The previous studies of the crystal perfection of other structures showed that the SH signal value in the maximum is higher for the structures with the high crystal perfection. In particular, the study [27] has revealed good match between the SH signal amplitude and the X-ray full width

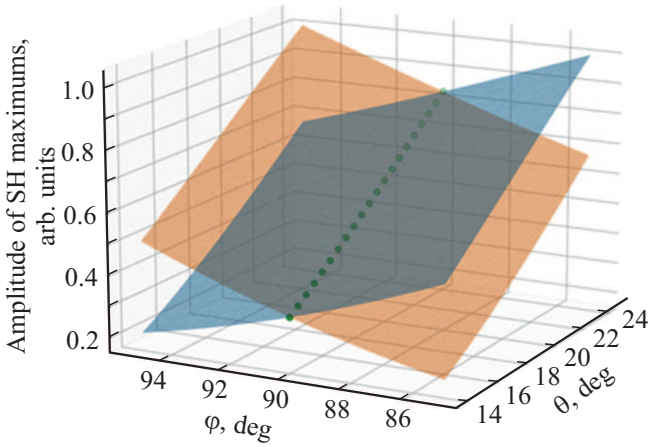

Figure 3. Behavior of the amplitudes of the two adjacent maxima for the azimutal curves of the SH signal around the (013) orientation depending on the angles θ and φ. The accurate orientation (013) is determined by angles $\theta \approx 19^\circ$ and $\varphi = 90^\circ$ (referenced from the (100) orientation).

at half-height (FWHM) for the structures grown at various ratios of the cadmium/tellurium fluxes. This confirms that the SH method can ensure the express sorting of the structures by the crystalline quality.

3.2. Results of the studying the (013)HgCdTe/CdTe/ZnTe/GaAs layer orientation of by the second harmonic generationand discussion

The SH studies showed that there was evidently the rotation of the crystal lattice φ within the (013) GaAs substrate plane and, subsequently, within the growth plane of the CdTe and HgCdTe surface layers inside the HgCdTe/CdTe/ZnTe/GaAs structure [26,27]. The determination accuracy of angle φ is ± 1 angl. deg. For the CdTe layers, the angle φ value is up to 8 angl. deg. from the (013)GaAs surface. For the MCT layers there was evidently non-monotonic variation of the angle φ throughout the thickness with insignificant reduction of the values in transition from the wide-band layers to absorber layers of the constant composition [24]. The structures 1MCT170622 and 1MCT180130 exhibit the change of the angle φ deviation from the ideal orientation (013) in the opposite directions, which is related to the surface polarity of GaAs substrates. The rotation of the layers orientation within the growth plane φ is related to screw dislocations [13,14]. The value of angle φ increases with the increase in the mismatch of the lattice parameters of conjugated materials, which for CdTe and GaAs is 13.6% and for CdTe and MCT $< 0.3\%$. The introduction of the dislocations, their density and the nature depend on the layer growth mechanism and their introduction into the growing layer. The observed variations φ qualitatively correspond to the variation of the lattice parameters mismatch and, consequently, to the mismatch dislocations density. With an increase in the lattice parameters mismatch, the dislocations density increases, thereby resulting in the increase of angle φ. When growing the MCT layers with the graded-gap wide-band layers, there is evidently the variation of the dislocations density, as shown by transmission electron microscopy [25]. There was evidently the introduction of the mismatch dislocations and subsequent formation of the dislocation net when growing the lower graded-gap wide-band MCT layer. The variation of the mismatch dislocations density results in the insignificant change of angle φ. With the increase in the MCT layer of constant composition, the dislocations density will remain the same and there is no change of angle φ. When growing the upper graded-gap wide-band MCT layer, the dislocations density is also changes in the same way as in growing the lower graded-gap wide-band layer, thereby resulting in the observed changed of angle φ and, correspondingly, in the rotation of the growing MCT layer orientation within the growth plane. For the quantitative dependence of angle φ, it is necessary to measure the screw dislocations density, which is difficult in some way. The SHG measurement of angle φ and

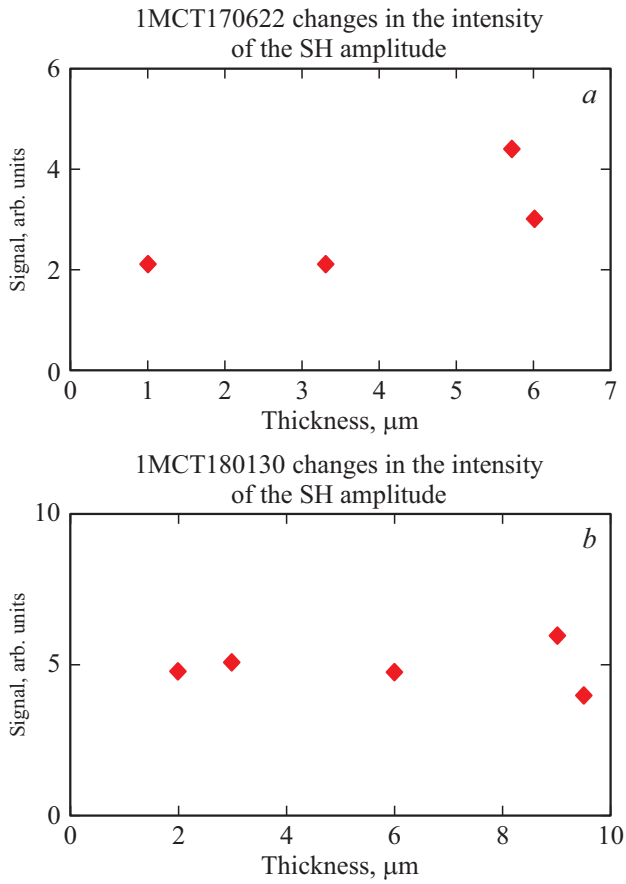

Figure 4. Dependence of the SH intensity throughout the thickness of the MCT layers in the MBE MCT HES structures: *a* — 1MCT170622; *b* — 1MCT180130.

the comparison with the condition of the layer growth in a complex multi-layer structure can be used for practical purposes when determining the optimum conditions of growing high-quality structures.

Fig. 4 shows the dependences of the relative SH amplitude intensity (the amplitude of the main maximum for the azimuthal dependence in relative units) throughout the layer thickness in the MBE MCT HES structures 1MCT170622 and 1MCT180130.

The change of the SH amplitude intensity with the same levels of exciting radiation 0.06 W and with the same reception path sensitivity is related to the change of angle θ, thereby characterizing the rotation of the orientation plane along the growth direction. As it follows from the given data, the SH amplitude intensity for the 1MCT170622 structure is 2 times less than for the 1MCT180130 structure. The SH amplitude intensity remains the same in the homogeneous MCT layer and increases on the surface of the upper graded-gap wide-band layer. Thus, angle θ has an almost constant value in the homogeneous MCT layer and increases to the upper graded-gap wide-band layer surface. Note that, in the 1MCT170622 structure when approaching the the upper wide-band graded-gap layer surface, in

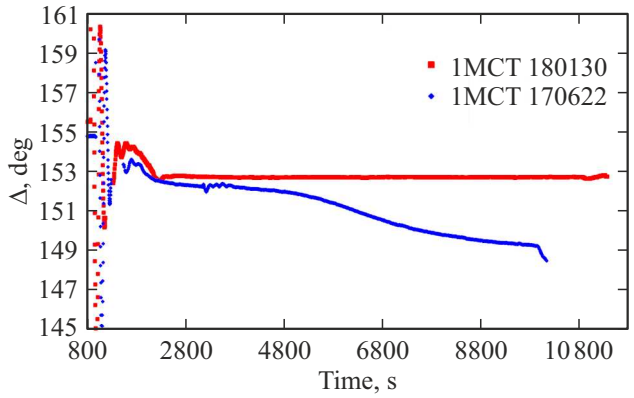

Figure 5. Dependence of the ellipsometry parameter Δ on the MCT layer growth time in the MBE MCT HES structures: blue rhombs — 1MCT170622; red squares — 1MCT180130.

accordance with the change of the SH amplitude, angle θ increases stronger in comparison with the 1MCT180130 structure, which is related to the non-optimum growth conditions of 1MCT170622. The rotation of the orientation plane long the growth direction in the similar MCT layers on the GaAs substrates was not observed when investigating by the X-ray diffraction, as it was shown in [25]. In fact, the dislocations density and the lattice parameters remain the same during the MCT layer growth of constant composition. Consequently, there is no motive force to ensure the rotation of the orientation during the growth. As it has been shown above, when growing the upper graded-gap wide-band layer, the dislocations density should change, and it should result in the observed variation of the angle θ and, consequently, in the rotation of the orientation along the growth direction. It is difficult to obtain this result when observing the rotation by the X-ray diffraction method. On the contrary, the SHG method, which makes it possible to probe thin near-surface layers, made it possible to show the observed changes in the angle θ from measurements of the intensity of the SH amplitude. The absolute angle θ value in the HgCdTe absorber layer for the 1MCT170622 structure is 8–10° lower than in the HgCdTe absorber layer for the 1MCT180130 structure, provided that structures have the same crystal perfection. Taking into account these data and considering the difference in the intensity of the SH amplitude for the studied structures, we can say that for the 1MCT170622 structure the crystal perfection of the HgCdTe layer is significantly lower than for the 1KPT180130 structure. Fig. 5 shows the experimental data for measuring the ellipsometry parameter Δ during growth of the 1MCT170622 and 1MCT180130 structures. The given data show various changes of this parameter, thereby indicating the growth of the structures in the various conditions. For 1MCT180130, there is evidently a typical variation of the values Δ when growing the MCT layer with the graded-gap wide-band layers. The parameter Δ remains the same when growing the layer of the homogeneous composition within the time interval 2300–10800 s, thereby indicating the optimum growth conditions (Fig. 5, red squares). On the contrary, for 1MCT170622, when growing the layer of the homogeneous composition, starting with 2300 s, there is evidently decrease of Δ and its sharp fall when growing the graded-gap wide-band layer, which is related to realizing the processes in the nonoptimal conditions (Fig. 5, blue rhombs). The decrease in the parameter Δ indicates a significant change of the surface morphology and its degradation in time, thereby preventing growing the thick layers. This difference in the growing of 1MCT170622 and 1MCT180130 must result in the different mechanisms of dislocation introduction during growing the graded-gap wide-band layer at the end of the growth process, taking to the analysis dislocations introduction when growing the (013)CdTe/ZnTe/GaAs structures [25].

Thus, by comparing the angle θ for the grown structures with the value of the angle θ for the HgCdTe reference specimen, it is possible to qualitatively evaluate the crystal perfection.

The analysis of the comparison of the above-given experimental data for the layer rotation dynamics of angles θ and φ throughout the heterostructure thickness allows unambiguously conclude that there is no relation in these rotations for angles θ and φ, i.e. the causes of the orientation variations for the angles θ and φ of the structure during the growth can be different and totally independent.

4. Conclusion

The structural perfection of the HgCdTe layers in the MBE MCT HES'es grown on the (013)GaAs substrate with the ZnTe and CdTe buffer layers at the azimuthal measurement of the second harmonic generation intensity was determined using the highly-sensitive test bench of the non-linear optical diagnostics. The experimental and calculation data have been compared. The calculation was performed based on the model azimuthal SH intensity dependence for the normal beam incidence at the variation of the orientation for angle φ near (013). The change of angle φ to 8 angle degree on the (013) orientation of the GaAs substrate determines the rotation of the orientation within the growth plane during growing the MBE MCT HES'es. The non-monotonic variation of the angle φ across the MCT layer thickness and its small increase in the graded-gap wide-band layers is related to the formation of the mismatch dislocations. In the layers of constant composition, angle φ remains the same, thereby indicating no rotation of the orientation in the growth plane. The analysis of the SH amplitude intensity allowed evaluating the change of angle θ when growing the MBE MCT HES'es, which showed its variation by 5 angle degree from the (013) orientation of the GaAs substrate. This variation is related to the rotation of the orientation along the growth direction. We relate the insignificant increase in the angle θ in the graded-gap wide-band layer to the variation in the density

of threading dislocations in its growing. The rotation of the surface orientation during the MBE MCT HES growth from the (013) orientation of the GaAs substrate is determined by the lattice parameters mismatch. The large mismatch of the lattice parameters for MCT and GaAs determines the significant rotation of the orientation within the growth plane and along its direction. The small mismatch of the lattice parameters during growing the MCT layer with changing the composition across the thickness determines insignificant changes of the orientation rotation within the growth plane and along its direction. The SH amplitude intensity value can be determined by the express method of determining the crystal perfection of the MCT layers.

Funding

The study was partially supported by the Russian Foundation for Fundamental Research (project No. 18-29-20053; the project No. 21-52-12015), Volkswagen Found, the project No. 97738, and as part of the state assignment of the Russian Federal Ministry of Education and Science in terms of project AAAA-A20-120102190007-5.

Conflict of interest

The authors declare that they have no conflict of interest.

References

[1] W. Lei, J. Antoszewski, L. Faraone. APR, **2**, 041303 (2015).
[2] V.S. Varavin, S.A. Dvoretskii, N.N. Mikhailov, V.G. Remesnik, I.V. Sabinina, Yu.G. Sidorov, V.A. Shvets, M.V. Yakushev, A.V. Latyshev. Optoelectron. Instrument. Proc., **56**, 456, (2020).
[3] S.A. Dvoretsky, N.N. Mikhailov, V.G. Remesnik, Yu.G. Sidorov, V.A. Shvets, D.G. Ikusov, V.S. Varavin, M.V. Yakushev, J.V. Gumenjuk-Sichevska, A.G. Golenkov, I.O. Lysiuk, Z.F. Tsybrii, A.V. Shevchik-Sheker, F.F. Sizov, A.V. Latyshev, A.L. Aseev. Opto-Electron. Rev., **27** (3), 282 (2019).
[4] M.A. Fadeev, V.V. Rumyantsev, A.M. Kadykov, A.A. Dubinov, A.V. Antonov, K.E. Kudryavtsev, S.A. Dvoretskii, N.N. Mikhailov, V.I. Gavrilenko, S.V. Morozov. Opt. Express, **26**, 12755 (2018).
[5] S. Ruffenach, A. Kadykov,V.V. Rumyantsev, J. Torres, D. Coquillat, D. But, S.S. Krishtopenko, C. Consejo, W. Knap, S. Winnerl, M. Helm, M.A. Fadeev, N.N. Mikhailov, S.A. Dvoretskii, V.I. Gavrilenko, S.V. Morozov, F. Teppe. APL Materials, **5** (3), 35503 (2017).
[6] L.A. Almeida, M. Groenert, J. Markunas, J.H. Dinan. J. Electron. Mater., **35** (6), 1214 (2006).
[7] R.J. Koestner, H.F.J. Schaake. J. Vac. Sci. Technol. A, **6**, 2834 (1988).
[8] V.S. Varavin, S.A. Dvoretsky, V.I. Liberman, N.N. Mikhailov, Yu.G. Sidorov. J. Cryst. Growth, **159**, 1161 (1996).
[9] A. Million, L.Di. Cioccio, J.P. Gailliard, J. Piaguet. J. Vac. Sci. Technol. A, **6**, 2813 (1988).
[10] T.T. Lam, C.D. Moore, R.L. Forrest, M.S. Goorsky, S.M. Johnson, D.B. Leonard, T.A. Strand, T.J. De Lyon, M.D. Gorwitz. J. Electron. Mater., **29** (6), 804 (2000).
[11] B. Shojaei, R. Cottier, D. Lee, E. Piquette, M. Carmody, M. Zandian, A. Yulius. J. Electron. Mater., **48** (10), 6118 (2019).
[12] T. Skauli, T. Colin, R. Sløtie, S. Løvold. J. Electron. Mater., **29** (6), 687 (2000).
[13] F. Riesz. J. Appl. Phys., **79**, 4111 (1996).
[14] C.C. Fulk, T. Parodos, P. Lamarre, S. Tobin, P. LoVecchio, J. Markunas. J. Electron. Mater., **38** (8), 1690 (2009)
[15] N. Nagai. J. Appl. Phys., **45**, 3789 (1974).
[16] P. Auvray, M. Baudet, A. Regreny. J. Cryst. Growth, **95**, 288 (1989).
[17] Y. Takagi, Yu. Furukawa, A. Wakahara, H. Kan. J. Appl. Phys., **107**, 063506 (2010).
[18] A.V. Kolesnikov, A.S. Ilin, E.M. Trukhanov, A.P. Vasilenko, I.D. Loshkarev, A.S. Deryabin. Bull. Russ. Acad. Sci. Phys., **75**, 609 (2011).
[19] I.D. Loshkarev, A.P. Vasilenko, E.M. Trukhanov, A.V. Kolesnikov, M.A. Putyato, B.R. Semyagin, V.V. Preobrazhenskii, O.P. Pchelyakov. Bull. Russ. Acad. Sci. Phys., **577**, 233 (2013).
[20] A.V. Kolesnikov, E.M. Trukhanov, A.S. Ilin, I.D. Loshkarev. J. Surf. Investig., **8**, 647 (2014).
[21] I.D. Loshkarev, A.P. Vasilenko, E.M. Trukhanov, A.V. Kolesnikov, M.A. Putyato, M.Yu. Esin, M.O. Petrushkov. Tech. Phys. Lett., **43**, 213 (2017).
[22] E.A. Emelyanov, A.V. Vasev, B.R. Semyagin, M.Yu. Yesin, I.D. Loshkarev, A.P. Vasilenko, M.A. Putyato, M.O. Petrushkov, V.V. Preobrazhenskii. Semiconductors **53**, 503 (2019).
[23] E. Ligeon, C. Chami, R. Danielou, G. Feuillet, J. Fontenelie, K. Seminadayar, A. Ponchet. J. Appl. Phys., **67**, 2428 (1990).
[24] W.F. Znhao, R.N. Jakobs, M. Jaime-Vasquez, L.O. Bubulak, D.J. Smith. J. Electron. Mater., **40** (8), 1733 (2011).
[25] Yu.G. Sidorov, M.V. Yakushev, V.S. Varavin, A.V. Kolesnikov, E.M. Trukhanov, I.V. Sabinina, I.D. Loshkarev. Phys. Solid State, **57**, 2151 (2015).
[26] M.F. Stupak, N.N. Mikhailov, S.A. Dvoretskii, M.V. Yakushev. Optoelectron.Instrument.Proc., **55**, 447 (2019).
[27] M.F. Stupak, N.N. Mikhailov, S.A. Dvoretskii, M.V. Yakushev. D.G. Ikusov, S.N. Makarov, A.G. Elesin, A.G. Verkhoglyad. Phys. Solid State, **62**, 252 (2020).
[28] M.F. Stupak, N.N. Mikhailov, S.A. Dvoretskiy, S.N. Makarov, A.G. Elesin, A.G. Verkhoglyad. ZhTF, **91** (11), 1799 (2021) (in Russian).
[29] S.A. Dvoretskii, M.F. Stupak, N.N. Mikhailov, S.N. Makarov, A.G. Elesin & A.G. Verkhoglyad. Optoelectron. Instrument. Proc., **57**, 458 (2021).
[30] S.A. Akhmanov, V.I. Emel'yanov, N.I. Koroteev, V.N. Seminogov. Sov. Phys. Usp., **28**, 1084 (1985).
[31] T.F. Heinz. *Second-Order Nonlinear Optical Effects at Surfaces and Interfaces*. In: *Nonlinear Surface Electromagnetic Phenomena*, eds by H. Ponath, G. Stegeman (North Holland Pub., Amsterdam, 1991).
[32] T. Kimura, Ch. Yamada. J. Cryst. Growth, **150**, 92 (1995).
[33] K.A. Brekhov, K.A. Grishunin, D.V. Afanas'ev, S.V. Semin, N.E. Sherstyuk, E.D. Mishina, A.V. Kimel. Phys. Solid State, **60**, 31 (2018).
[34] V.V. Balanyuk, V.F. Krasnov, S.L. Musher, V.I. Prots, V.E. Ryabchenko, S.A. Stoyanov, S.G. Strutsa, M.F. Stupak, V.S. Syskin. Quantum Elecronic, **25**, 183 (1995).
[35] G.M. Borisov, V.G. Gol'dort, A.A. Kovalev, S.A. Kochubey, D.V. Ledovskikh, V.V. Preobrazhenskiy, M.A. Putyato, N.N. Rubtsova, B.R. Semyagin. Vestn. Novosib. gos. un-ta. Ser. Fizika, **9** (4), 5 (2014) (in Russian).

[36] G.M. Borisov, V.G. Gol'dort, K.S. Zhuravlev, A.A. Kovalev, S.A. Kochubey, D.V. Ledovskikh, T.V. Malin, N.N. Rubtsova. Sibirskiy fiz. zhurn., **13** (2), 64 (2018) (in Russian).
[37] S.B. Bodrov, A.I. Korytin, Yu.A. Sergeev, A.N. Stepanov. Quantum Elecronic, **50**, 496 (2020).
[38] I.D. Burlakov, A.V. Demin, G.G. Levin, N.A. Piskunov, S.V. Zabotnov, A.S. Kashuba. Meas. Tech., **53**, 615 (2010).
[39] Y.V. Permikina, A.S. Kashuba. Uspekhi prikl. fiziki, **4** (5), 493 (2016) (in Russian).
[40] N.A. Kulchitskii. J. Commun. Technol. Electron. **67**, 324 (2022).
[41] Yu.G. Sidorov, S.A. Dvoretskii, V.S. Varavin, N.N. Mikhailov, M.V. Yakushev, and I.V. Sabinina. Semiconductors, **35**, 1045 (2001).
[42] V.I. Gavrilenko, A.M. Grekhov, D.V. Korbutyak, V.G. Litovchenko. *Opticheskiye svoistva poluprovodnikov*. Spravochnik (Kiev, Nauk. dumka, 1987) (in Russian).
[43] *Handbook of Optical Constants of Solids*, ed. by E.D. Palik (Elsevier Science, USA, 1998).
[44] Sadao Adachi. *Optical Constants of Crystalline and Amorphous Semiconductors* (Springer Science+Business Media, N.Y., 1999).
[45] E.D. Mishina, T.V. Misuryaev, N.E. Sherstyuk, V.V. Lemanov, A.L. Morozov, A.S. Sigov, Th. Rasing. Phys. Rev. Lett., **85** (17), 3664 (2000).
[46] E.D. Mishina, A.I. Morozov, A.S. Sigov, N.E. Sherstyuk, O.A. Aktsipetrov, V.V. Lemanov. J. Exp. Theor. Phys. **94**, 552 (2002).